Lasers Med Sci (2013) 28:851–858
DOI 10.1007/s10103-012-1170-8

ORIGINAL ARTICLE

Reliability evaluation of alumina-blasted/acid-etched versus laser-sintered dental implants

Erika O. Almeida · Amilcar C. Freitas Júnior · Estevam A. Bonfante · Nelson R. F. A. Silva · Paulo G. Coelho

Received: 7 December 2011 / Accepted: 16 July 2012 / Published online: 28 July 2012

Abstract Step-stress accelerated life testing (SSALT) and fractographic analysis were performed to evaluate the reliability and failure modes of dental implant fabricated by machining (surface treated with alumina blasting/acid etching) or laser sintering for anterior single-unit replacements. Forty-two dental implants (3.75×10 mm) were divided in two groups (n=21 each): laser sintered (LS) and alumina blasting/acid etching (AB/AE). The abutments were screwed to the implants and standardized maxillary central incisor metallic crowns were cemented and subjected to SSALT in water. Use-level probability Weibull curves and reliability for a mission of 50,000 cycles at 200 N were calculated. Polarized light and scanning electron microscopes were used for failure analyses. The Beta (β) value derived from use-level probability Weibull calculation of 1.48 for group AB/AE indicated that damage accumulation likely was an accelerating factor, whereas the β of 0.78 for group LS indicated that load alone likely dictated the failure mechanism for this group, and that fatigue damage did not appear to accumulate. The reliability was not significantly different (p>0.9) between AB/AE (61 %) and LS (62 %). Fracture of the abutment and fixation screw was the chief failure mode. No implant fractures were observed. No differences in reliability and fracture mode were observed between LS and AB/AE implants used for anterior single-unit crowns.

Keywords Dental implant · Reliability · Laser solid-state · Step-stress accelerated life testing · Weibull analysis

E. O. Almeida · A. C. F. Júnior · P. G. Coelho
Department of Biomaterials and Biomimetics,
New York University,
345E, 24th Street,
New York, NY 10010, USA

E. A. Bonfante (✉)
Postgraduate Program in Dentistry,
UNIGRANRIO University—School of Health Sciences,
Rua Prof. José de Souza Herdy, 1.160, 25 de Agosto,
Duque de Caxias, RJ, Brazil 25071-202
e-mail: estevamab@gmail.com

N. R. F. A. Silva
Department of Operative Dentistry,
Federal University of Minas Gerais-UFMG,
Belo Horizonte, MG 31270-901, Brazil

P. G. Coelho
Department of Periodontology and Implant Dentistry,
Director for Research, New York University College of Dentistry,
345 E, 24th Street,
New York, NY 10010, USA

Introduction

It is general consensus that rough implant surfaces are more osteoconductive than smooth surfaces, [1–3] and result in high long-term survival and success rates [4–6]. Surface texturing is commonly employed as one of the final steps prior to cleaning, packaging, and sterilizing dental implants, and such procedures may have drawbacks such as increased final cost and potential implant contamination with blasting media and organic contaminants from surface processing which may jeopardize osseointegration [7]. Thus, alternative methods which allow surface texturing during the manufacturing process are desirable.

The laser metal-sintering process is a technology that produces solid metal components with intricate porous geometries [1, 2]. Potential advantages of laser sintering is high throughput manufacturing along with potential improved properties such as the elastic properties that may be tailored to more closely match those of bone [2, 8], potentially improving the bone–implant complex biomechanics

[9, 10]. Advantages also include that implants may be manufactured from commercially pure titanium or alloys [8].

From a host response to laser-sintered implants perspective, a previous study have demonstrated acceptable osseointegration levels to laser-modified implants relative to alumina-blasted/acid-etched implants, along with different fracture patterns between the interface and bone following mechanical testing [11, 12]. Transmission electron microscopy and chemical analysis showed coalescence between mineralized tissue and the surface of the laser-modified implant [13]. Recently, improved biomechanical response has been reported for laser-sintered compared to alumina-blasted/acid-etched implants at early times (1 and 6 weeks in vivo) [14]. A human retrieval study [8] showed that the laser-sintered surface presented a close contact with the bone after 8 months in vivo. However, it is unclear if the laser sintering alters the mechanical behavior of the implant. While the biocompatibility of implants fabricated by the laser-sintering process has been demonstrated [1], limitations that are inherent to sintering processes such as the potential for flaws in the material surface and bulk has raised concerns when it comes to their mechanical performance.

Several testing methods have been described for the mechanical evaluation of implant systems, such as single load to fracture [15], the use fatigue followed by the application of a static load until fracture [16, 17], the staircase method [18], fatigue limit (ISO 14801:2007), step-stress accelerated life testing [19], and others. While the ISO 14801:2007 was created with the aim to standardize the testing procedures and data presentation in fatigue of dental implants, it has been shown that results produced by such method should be interpreted with caution. The wide range of testing parameters allowed in the ISO 14801:2007 regarding testing frequency (2–15 Hz), environment (water or dry when testing above 15 Hz), and amount of cycles (2 or 5 million, depending on chosen frequency) have shown that a very different failure probability distribution may result [20] as well as failure modes (transgranular in dry compared to intergranular in wet conditions) [21]. In addition, testing of one sample could take 12 days when carried on 2 Hz. Therefore, while attending industry requirements for implants quality assurance and control, the ISO 14801:2007 testing methodology seems to be under development since its first version in 2003 [20, 21].

In attempt to reduce testing times, accelerated life testing may be designed to cause products to fail more quickly and yet with realistic failure mechanisms compared to failures under use stress. Qualitative or quantitative accelerated tests may be used to describe failure modes or estimate the probability density function, respectively, for the product under normal use conditions, with common use in the military, electrical, mechanical engineering, and many other fields. Then, using data obtained during testing at different accelerated stress levels, commonly used life distributions, such as Exponential, Lognormal, or Weibull may be used to estimate the parameters that best fits the data.

The use of accelerated life tests in dental research has been reported in a series of studies concerning the reliability of a variety of prosthetic restorative systems where a remarkable resemblance between the resulting failure modes was observed when compared to clinical failures [22–25]. Similar findings were reported when accelerated life tests were used in implant-borne reconstructions [19]. Considering the unknown mechanical performance of direct laser metal sintering as a process for implant fabrication, the aim of this study was to evaluate the reliability and failure modes of anatomically correct maxillary central incisor crowns as a function of supporting titanium implant structure (laser sintered vs alumina blasted/acid etched). The postulated hypothesis was that different fabrication methods would result in different reliability and failure modes when subjected to step-stress accelerated life testing (SSALT) in water.

Materials and methods

Sample preparation

Forty-two dental implants (3.75 mm diameter by 10 mm length, internal connection; A.B. Dental Devices Ltd., Ashdod, Israel) were divided in two groups ($n=21$) according to the fabrication method: laser-sintered implant (LS, Figs. 1a, b and 2a) and machining followed by alumina-blasting/acid-etching surface treatment (AB/AE; Figs. 1c, d and 2b). All implants were vertically embedded in acrylic resin (Orthoresin, Degudent, Mainz, Germany), poured in a 25-mm-diameter plastic tube, leaving the top platform in the same level of the potting surface.

A maxillary central incisor crown was waxed to its close anatomical shape and cast in CoCr metal alloy (cobalt–chrome partial denture alloy, BEGO, Bremen, Germany). In order to reproduce the anatomy of the crowns, an impression was taken from the first waxed pattern and used by the technician as a guide during waxing of the remaining crowns. The prefabricated abutments (Ti-6Al-4V) were torqued with a torque gauge according to the manufacturer's instructions (30 Ncm; A.B. Dental Devices Ltd. Ashdod, Israel). Following connection, the cementation surface of the crowns was blasted with aluminum oxide (particle size ≤40 μm, using 276 KPa compressed air pressure), cleaned with ethanol, dried with air free of water and oil, and then cemented (Rely X Unicem, 3M ESPE, St. Paul, USA; Fig. 2c, d).

Mechanical testing and reliability analysis

For mechanical testing, the specimens were subjected to 30° off-axis loading (Fig. 2e). Three specimens of each group

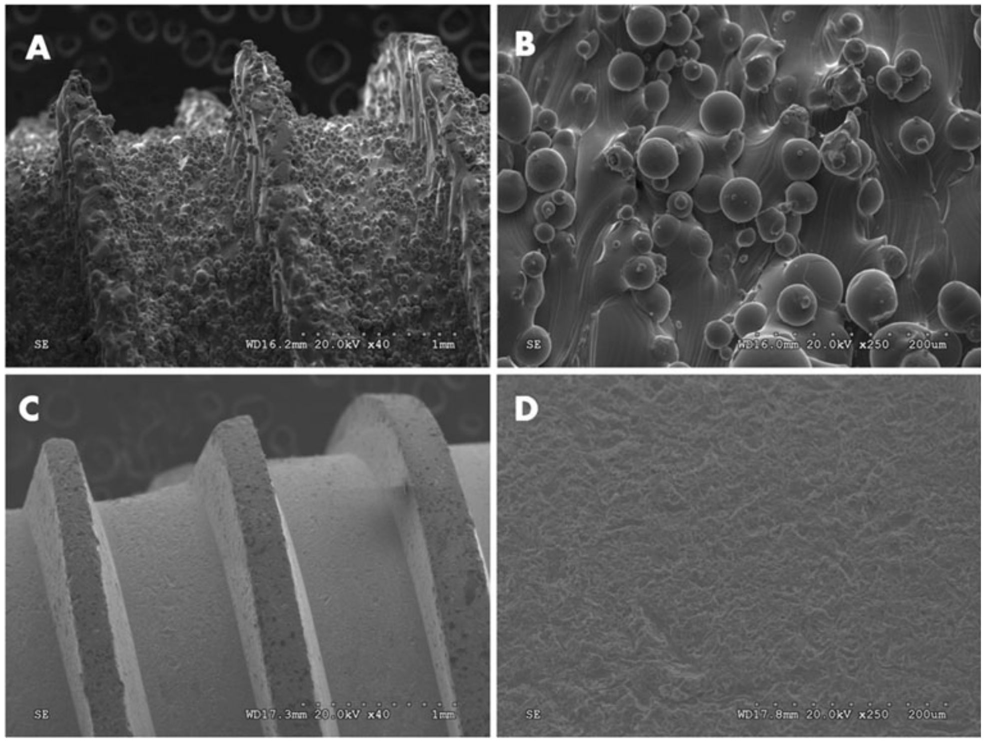

Fig. 1 SEM micrographs of the threads of laser sintered (**a** and **b**) and alumina-blasted/acid-etched (**c** and **d**) implants where differences in roughness and porosities are noticeable. The laser-sintered implant depicts an irregular surface with ridged-like and globular protrusions, interspersed by intercommunications by irregular crevices (**a** and **b**)

underwent single-load-to-failure (SLF) testing at a cross-head speed of 1 mm/min in a universal testing machine (INSTRON 5666, Canton, MA, USA) with a flat tungsten carbide indenter applying the load at the incisal edge of the crown. Based upon the mean load to failure from SLF, three step-stress accelerated life-testing profiles were determined for the remaining 18 specimens of each group which were assigned to a mild (n=9), moderate (n=6), and aggressive (n=3) fatigue profiles (ratio 3:2:1, respectively) [26]. These profiles are named based on the step-wise load increase that the specimen will be fatigued throughout the cycles until a certain level of load, meaning that specimens assigned to a mild profile will be cycled longer to reach the same load level of a specimen assigned to the aggressive profile [27].

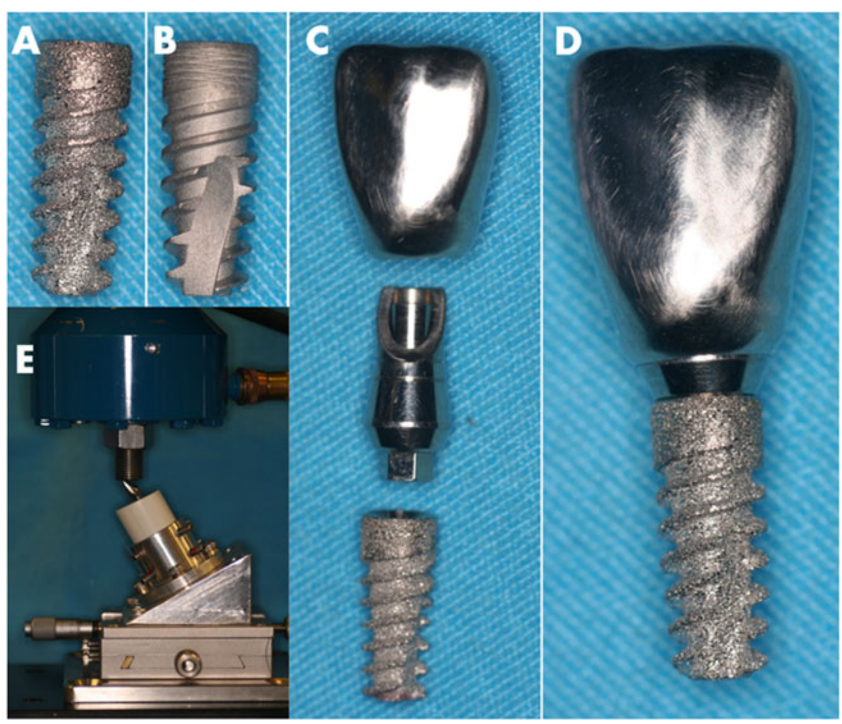

Fig. 2 **a** Laser-sintered and **b** alumina-blasted/acid-etched implant; **c** maxillary central incisor metallic crown, internally connected abutment and laser-sintered implant; **d** components assembled after abutment torque and crown cementation in a laser-sintered sample; **e** mechanical testing set up, where the load was applied at 30° to the long axis of the implant

The prescribed fatigue method was step-stress accelerated life-testing under water at 9 Hz with a servo-all-electric system (TestResources 800L, Shakopee, MN, USA) where the indenter contacted the incisal edge, applied the prescribed load within the step profile and lifted off the incisal edge. Fatigue testing was performed until failure (bending or fracture of the fixation screw, and/or bending, partial fracture, or total fracture of the abutment) or survival (no failure occurred at the end of step-stress profiles, where maximum loads were up to 600 N) [19].

Use level probability Weibull curves (probability of failure versus number of cycles) with a power law relationship for damage accumulation were calculated (Alta Pro 7, Reliasoft, Tucson, AZ, USA) [28]. The two-parameter Weibull probability density function is given by:

$$f(T) = \frac{\beta}{\eta}\left(\frac{T}{\eta}\right)^{\beta-1} e^{-\left(\frac{T}{\eta}\right)^{\beta}} \tag{1}$$

where: $f(T) \geq 0$, $T \geq 0$, $\beta 0$, $\eta 0$ and η=scale parameter/ β=shape parameter (or slope)

If the use level probability Weibull calculated beta (β is the slope of the regressed line in a probability plot and describes the reliability and failure rate functions) was less than 1 for any group (meaning that the implant–abutment connection failure is controlled by materials strength rather than damage accumulation from fatigue testing),[29] then a Weibull two-parameter Contour plot (Weibull modulus (m) versus characteristic strength (η, i.e., which indicates the load at which 63.2 % of the specimens of each group would fail)) was calculated (Weibull 7++, Reliasoft, Tucson, Arizona, USA) using final load at failure or survival of specimens as input [27, 30]. The calculated Weibull modulus (m) and characteristic strength Eta (η; 63.2 % of the specimens would fail up to the calculated "η") values were utilized to determine the confidence bounds through the maximum likelihood ratio method utilizing a chi-squared value at 95 % level of significance and 1 degree of freedom. Thus, each contoured region represent possible values given both parameters combination, and significant difference at 95 % level is detected if contour overlap between groups does not exist (in such case, samples will be considered to be from different populations) [27, 31]. The reliability (the probability of an item functioning for a given amount of time without failure) for a mission of 50,000 cycles at 200 N load [32] (two-sided 95 % confidence intervals) was calculated for comparison between AB/AE and LS. For the mission reliability and β parameters calculated in the present study, the 95 % confidence interval range were calculated as follows: CB=$E(G)\pm z_{\alpha}$ sqrt(Var(G)), where: CB is the confidence bound, $E(G)$ is the mean estimated reliability for the mission calculated from Weibull statistics, z_{α} is the z value concerning the given CI level of significance, and Var(G) is the value calculated by the Fisher Information matrix [27, 31].

Failure analysis

Images of failed samples were taken with macro lens attached to a digital camera (Canon EOS, Macro 110, New York, NY, USA) and utilized for failure mode classification and comparisons between groups. In order to identify fractographic markings and characterize failure origin and propagation direction, the most representative failed samples of each group were inspected first under a polarized-light microscope (MZ-APO stereomicroscope, Carl Zeiss MicroImaging, Thornwood, NY, USA) and then by scanning electron microscopy (SEM; Model S-3500N, Hitachi, Osaka, Japan) [33].

Results

SLF and reliability

The SLF mean ± standard deviation values for the group AB/AE were 355±31 N, and 652±251 N for the group LS.

The step-stress derived probability Weibull plots and summary statistics at a 200-N load are presented in Fig. 3a and Table 1. The Beta (β) value mean (95 % confidence interval range) derived from use level probability Weibull calculation (probability of failure vs. number of cycles) of 1.48 (0.80–2.74) for group AB/AE indicated that fatigue was an accelerating factor (damage accumulation). On the other hand, the resulting β of 0.78 (0.43–1.41) for group LS indicated that load alone dictated the failure mechanism for this group, and that fatigue damage did not appear to accumulate.

Load-at-failure data of the two groups was then used to calculate the probability Weibull distribution. which showed a m=10.0 for the group AB/AE and m=9.8 for the group LS, and characteristic strength of η=246.1 N for AB/AE and η=243.9 N for LS. The confidence bounds calculated through the likelihood ratio method at 95 % level of significance represented by the contours in Fig. 3b showed that the groups were statistically homogenous (p>0.9; confidence interval overlap) [27, 30].

The step-stress accelerated fatigue permit estimates of reliability at a given load level (Table 1). The calculated reliability with 95 % confidence intervals for a mission of 50,000 cycles at 200 N showed that the cumulative damage from loads reaching 200 N would lead to implant-supported restoration survival in 61 % for group AB/AE and 62 % for LS. The overlap between the upper and lower limits of reliability values in groups AB/AE and LS indicates no statistically significant difference (Table 1).

Failure modes

All specimens failed after SSALT. When component failures were evaluated together, failures comprised the combination

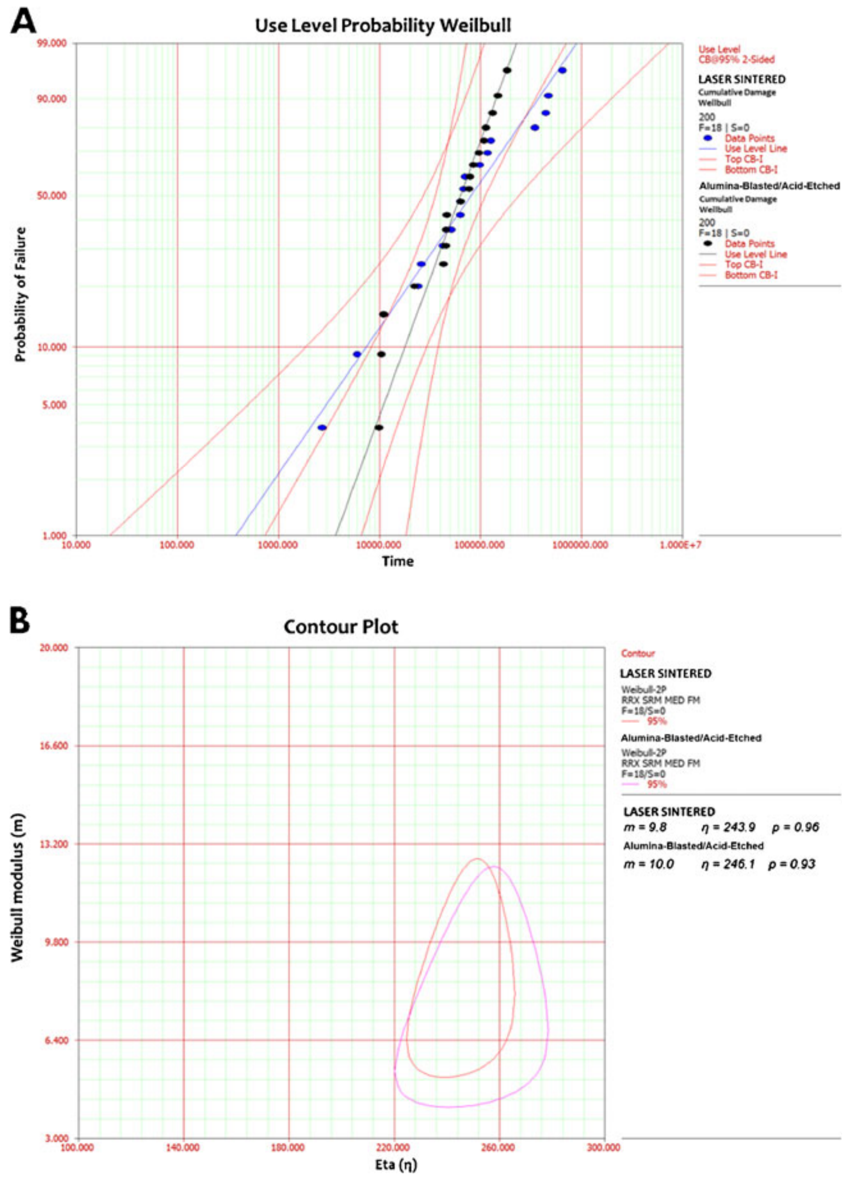

Fig. 3 **a** Use level probability Weibull for tested groups showing the probability of failure as a function of number of cycles (time) given a mission of 50,000 cycles at 200 N. **b** Contour plot (Weibull modulus vs characteristic strength) for group comparisons (laser-sintered and alumina-blasted/acid-etched implant). Note the overlap between groups indicating the absence of statistical significance

of screw and abutment fracture. Failure modes are presented in Fig. 4.

For both AB/AE and LS groups, fracture at the interface between the abutment and the implant was the chief failure mode (Fig. 4). In all specimens from both groups, the abutment and the fixation screw fractured (Figs. 4c and 5), but the implants were intact after mechanical testing.

Table 1 Calculated reliability for laser-sintered and alumina-blasted/acid-etched implants used to support maxillay central incisors given a mission of 50,000 cycles at 200 N load

Output (50,000 cycles at 200 N)	AB/AE	LS
Upper	0.80	0.80
Reliability	0.61	0.62
Lower	0.34	0.35
Beta	1.48 (0.80–2.74)	0.78 (0.43–1.41)

Polarized-light and SEM micrographs of the fractured surface of fixation screws and abutments allowed the consistent identification of fractographic features, such as compression curl (CC), which allowed the identification of fracture origin and the direction of crack propagation (Fig. 5b, e). Figure 5c also depicts the dimpled appearance of the abutment screw typical of ductile fracture of metallic materials [34].

Discussion

The majority of published data concerning evaluation of implants fabricated by different methods (alumina-blasted/acid-etched and laser-sintered implants) have focused on the

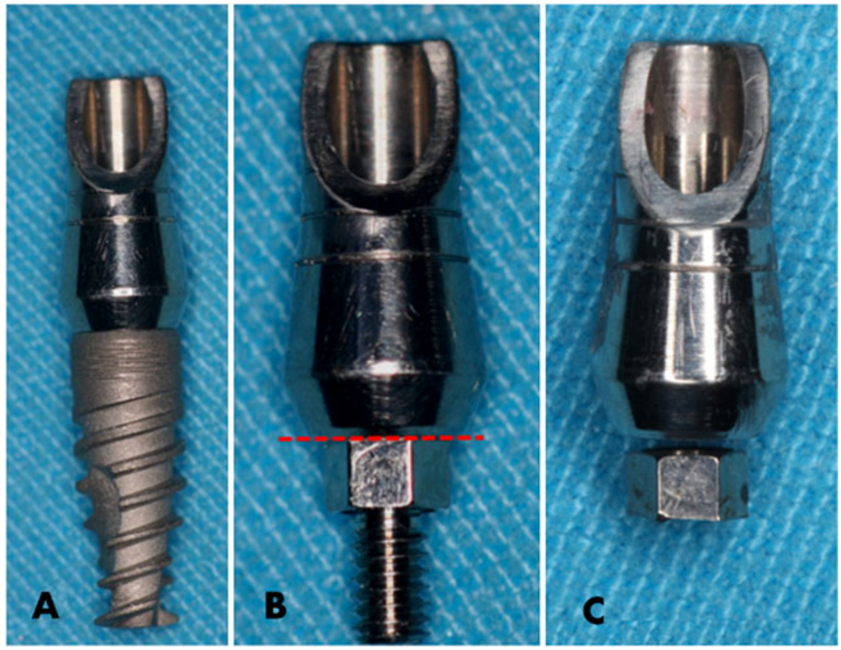

Fig. 4 **a** Abutment and alumina-blasted/acid-etched implant assembly; **b** representative region of fracture of the abutment and abutment screw; **c** fractured abutment

biomechanical testing in in vivo laboratory animal model. These studies reported an increase in removal torque for the laser-treated titanium implants compared to implants that were fabricated by machining [35–37]. Such results are likely due to the higher surface roughness and thereby mechanical interlocking between bone and laser-sintered/textured implants compared to implants that are first machined and then textured by a variety of methods (Coelho et al. 2008). Other studies have also shown acceptable osseointegration of laser-treated surfaces [8, 13]. Since previous work has reported the appropriate biocompatible and osseoconductive properties of laser-treated and laser-sintered implants, the present study aimed to investigate whether laser-sintered fabricated implants would present different reliability and failure modes compared to current industry standard alumina-blasted/acid-etched implant.

The scenario simulated in the present study represented a common clinical situation for single-tooth replacements in anterior region of maxilla. The specimens were subjected to step-stress accelerated fatigue test in water, which has been suggested as an important service-related cause of failure in metals [34]. Our results showed similar fatigue endurance for both alumina-blasted/acid-etched and laser-sintered implants. On the other hand, the resulting β value (called the Weibull shape factor) of 1.48 for group AB/AE and of 0.78 for group LS indicated that damage accumulation

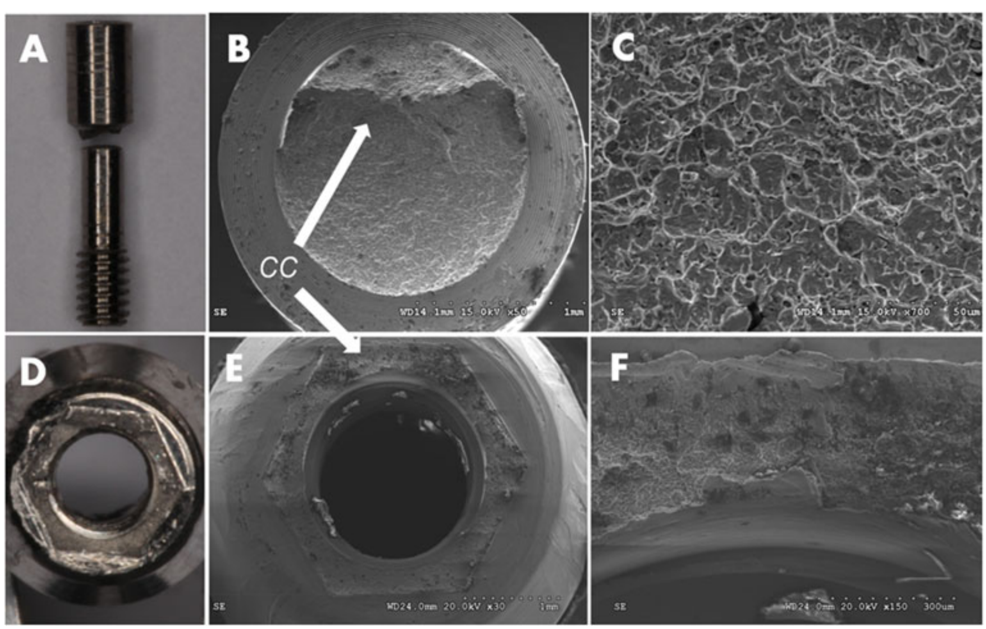

Fig. 5 **a** Macro picture of the abutment screw and **d** fractured abutment; SEM micrograph of (**b** and **c**) fractured abutment screw and (**d** and **e**) the abutment surfaces. **b** and **e** The *white arrows* shows a compression curl (*CC*), which allowed the identification of direction of crack propagation. **c** Dimpled surface appearance of the abutment screw fractured surface

influenced in implant-supported restoration failure only for AB/AE surface implants. The β value describes failure rate changes over time (β<1: failure rate is decreasing over time, commonly associated with "early failures" or failures that occur due to egregious flaws; β~1: failure rate that does not vary over time, associated with failures of a random nature; β>1: failure rate is increasing over time, associated with failures related to damage accumulation) [26, 38].

In the present study, the region of fracture in all specimens was between the abutment and implant platform for both AB/AE and LS groups. Thus, it may be assumed that the abutment and fixation screw fractured together, and the implant was the strongest component of the implant–abutment connection regardless of implant fabrication method. These findings suggest that the laser-sintered titanium implant surface did not affect the implant fatigue endurance. This is of special interest considering that although implant fracture may not be a commonly reported failure, it must be acknowledged that available clinical studies mainly involve follow-ups from 5 to 10 years [39–44]. Longer clinical observations of 15 years for instance have reported implant fractures mainly occurring after 5 years of occlusal function resulting in an incidence of 3.5 % [45]. As implants are expected to survive long periods it becomes crucial to understand the fatigue mechanical behavior of implant systems fabricated by different methods.

Considering that the replacement of single-unit edentulous spaces in the anterior region of maxilla with implant-supported restorations is a challenging scenario in terms of mechanics and esthetics for the long-term success [46], every effort (such as laser technology) to improve the bone-to-implant contact is desirable. Therefore further studies, especially in vivo investigations related to biomechanical aspects of laser-sintered implants are warranted.

Conclusion

The postulated hypothesis that different implant fabrication methods result in different reliability and failure modes when subjected to step-stress accelerated life testing was rejected. When varying the implant fabrication method, no significant differences were observed in values of reliability after SSALT.

Acknowledgments The authors are thankful to *A.B. Dental Devices Ltd*. (Ashdod, Israel) and *Marotta Dental Studio* (Farmingdale, NY, USA) for their support.

References

1. Mangano C, Raspanti M, Traini T, Piattelli A, Sammons R (2009) Stereo imaging and cytocompatibility of a model dental implant surface formed by direct laser fabrication. J Biomed Mater Res A 88(3):823–831. doi:10.1002/jbm.a.32033
2. Traini T, Mangano C, Sammons RL, Mangano F, Macchi A, Piattelli A (2008) Direct laser metal sintering as a new approach to fabrication of an isoelastic functionally graded material for manufacture of porous titanium dental implants. Dent Mater 24 (11):1525–1533. doi:10.1016/j.dental.2008.03.029
3. Mangano C, Mangano F, Shibli JA, Luongo G, De Franco M, Briguglio F, Figliuzzi M, Eccellente T, Rapani C, Piombino M, Macchi A (2011) Prospective clinical evaluation of 201 direct laser metal forming implants: results from a 1-year multicenter study. Lasers Med Sci. doi:10.1007/s10103-011-0904-3
4. Romeo E, Lops D, Margutti E, Ghisolfi M, Chiapasco M, Vogel G (2004) Long-term survival and success of oral implants in the treatment of full and partial arches: a 7-year prospective study with the ITI dental implant system. Int J Oral Maxillofac Implants 19(2):247–259
5. Khayat PG, Milliez SN (2007) Prospective clinical evaluation of 835 multithreaded tapered screw-vent implants: results after two years of functional loading. Journal Oral Implantol 33(4):225–231. doi:10.1563/1548-1336(2007)33[225:PCEOMT]2.0.CO;2
6. Astrand P, Engquist B, Dahlgren S, Grondahl K, Engquist E, Feldmann H (2004) Astra Tech and Branemark system implants: a 5-year prospective study of marginal bone reactions. Clin Oral Implants Res 15(4):413–420. doi:10.1111/j.1600-0501.2004.01028.x
7. Coelho PG, Granjeiro JM, Romanos GE, Suzuki M, Silva NR, Cardaropoli G, Thompson VP, Lemons JE (2009) Basic research methods and current trends of dental implant surfaces. J Biomed Mater Res B Appl Biomater 88(2):579–596. doi:10.1002/jbm.b.31264
8. Mangano C, Piattelli A, Raspanti M, Mangano F, Cassoni A, Iezzi G, Shibli JA (2011) Scanning electron microscopy (SEM) and X-ray dispersive spectrometry evaluation of direct laser metal sintering surface and human bone interface: a case series. Lasers Med Sci 26(1):133–138. doi:10.1007/s10103-010-0831-8
9. Frenkel SR, Simon J, Alexander H, Dennis M, Ricci JL (2002) Osseointegration on metallic implant surfaces: effects of microgeometry and growth factor treatment. J Biomed Mater Res 63 (6):706–713. doi:10.1002/jbm.10408
10. Soboyejo WO, Nemetski B, Allameh S, Marcantonio N, Mercer C, Ricci J (2002) Interactions between MC3T3-E1 cells and textured Ti6Al4V surfaces. J Biomed Mater Res 62(1):56–72. doi:10.1002/jbm.10221
11. Oyonarte R, Pilliar RM, Deporter D, Woodside DG (2005) Peri-implant bone response to orthodontic loading: Part 1. A histomorphometric study of the effects of implant surface design. Am J Orthod Dentofacial Orthop 128(2):173–181. doi:10.1016/j.ajodo.2004.02.023
12. Pilliar RM, Sagals G, Meguid SA, Oyonarte R, Deporter DA (2006) Threaded versus porous-surfaced implants as anchorage units for orthodontic treatment: three-dimensional finite element analysis of peri-implant bone tissue stresses. Int J Oral Maxillofac Implants 21(6):879–889
13. Palmquist A, Emanuelsson L, Branemark R, Thomsen P (2011) Biomechanical, histological and ultrastructural analyses of laser micro- and nano-structured titanium implant after 6 months in rabbit. J Biomed Mater Res B Appl Biomater 97(2):289–298. doi:10.1002/jbm.b.31814
14. Witek L, Marin C, Granato R, Bonfante EA, Campos F, Bisinotto J, Suzuki M, Coelho PG (2012) Characterization and in vivo evaluation of laser sintered dental endosseous implants in dogs. J Biomed Mater Res B Appl Biomater. doi:10.1002/jbm.b.32725
15. Al-Omari WM, Shadid R, Abu-Naba'a L, El Masoud B (2010) Porcelain fracture resistance of screw-retained, cement-retained, and screw-cement-retained implant-supported metal ceramic posterior crowns. J Prosthodont 19(4):263–273. doi:10.1111/j.1532-849X.2009.00560.x

16. Dittmer MP, Dittmer S, Borchers L, Kohorst P, Stiesch M (2011) Influence of the interface design on the yield force of the implant–abutment complex before and after cyclic mechanical loading. J Prosthodont Res. doi:10.1016/j.jpor.2011.02.002
17. Kohal RJ, Wolkewitz M, Tsakona A (2011) The effects of cyclic loading and preparation on the fracture strength of zirconium-dioxide implants: an in vitro investigation. Clin Oral Implants Res 22(8):808–814. doi:10.1111/j.1600-0501.2010.02067.x
18. Ribeiro CG, Maia ML, Scherrer SS, Cardoso AC, Wiskott HW (2011) Resistance of three implant-abutment interfaces to fatigue testing. J Appl Oral Sci 19:413–420
19. Freitas AC Jr, Bonfante EA, Rocha EP, Silva NR, Marotta L, Coelho PG (2011) Effect of implant connection and restoration design (screwed *vs.* cemented) in reliability and failure modes of anterior crowns. Eur J Oral Sci 119(4):323–330. doi:10.1111/j.1600-0722.2011.00837.x
20. Karl M, Kelly JR (2009) Influence of loading frequency on implant failure under cyclic fatigue conditions. Dent Mater 25 (11):1426–1432. doi:10.1016/j.dental.2009.06.015
21. Lee CK, Karl M, Kelly JR (2009) Evaluation of test protocol variables for dental implant fatigue research. Dent Mater 25 (11):1419–1425. doi:10.1016/j.dental.2009.07.003
22. Coelho PG, Bonfante EA, Silva NR, Rekow ED, Thompson VP (2009) Laboratory simulation of Y-TZP all-ceramic crown clinical failures. J Dent Res 88(4):382–386. doi:10.1177/0022034509333968
23. Silva NR, Bonfante EA, Zavanelli RA, Thompson VP, Ferencz JL, Coelho PG (2010) Reliability of metalloceramic and zirconia-based ceramic crowns. J Dent Res 89(10):1051–1056. doi:10.1177/0022034510375826
24. Guess PC, Zavanelli RA, Silva NR, Bonfante EA, Coelho PG, Thompson VP (2010) Monolithic CAD/CAM lithium disilicate versus veneered Y-TZP crowns: comparison of failure modes and reliability after fatigue. Int J Prosthodont 23(5):434–442
25. Bonfante EA, Coelho PG, Navarro JM Jr, Pegoraro LF, Bonfante G, Thompson VP, Silva NR (2010) Reliability and failure modes of implant-supported Y-TZP and MCR three-unit bridges. Clin Implant Dent Relat Res 12(3):235–243. doi:10.1111/j.1708-8208.2009.00156.x
26. Coelho PG, Silva NR, Bonfante EA, Guess PC, Rekow ED, Thompson VP (2009) Fatigue testing of two porcelain-zirconia all-ceramic crown systems. Dent Mater 25(9):1122–1127. doi:10.1016/j.dental.2009.03.009
27. Abernethy R (2006) The new Weibull handbook, 5th edn. Dr. Robert B. Abernethy, North Palm Beach
28. Zhao WE (2005) A general accelerated life model for step-stress testing. IEEE Trans Reliabil 37:1059–1069
29. Reliasoft (2010) The Weibull Distribution and Beta. http://www.weibull.com/hotwire/issue110/hottopics110.htm
30. Nelson W (1990) Accelerated testing: statistical models, test plans and data analysis. Wiley, New York
31. Nelson W (2004) Accelerated testing: statistical models, test plans and data analysis. Wiley, New York
32. Hellsing G (1980) On the regulation of interincisor bite force in man. J Oral Rehabil 7(5):403–411
33. Manda MG, Psyllaki PP, Tsipas DN, Koidis PT (2009) Observations on an in-vivo failure of a titanium dental implant/abutment screw system: a case report. J Biomed Mater Res B Appl Biomater 89(1):264–273. doi:10.1002/jbm.b.31211
34. Parrington R (2002) Fractography of metals and plastics In: Park M (ed) Practical Failure Analysis. ASM International. 2(5):16–22
35. Rong M, Zhou L, Gou Z, Zhu A, Zhou D (2009) The early osseointegration of the laser-treated and acid-etched dental implants surface: an experimental study in rabbits. J Mater Sci Mater Med 20(8):1721–1728. doi:10.1007/s10856-009-3730-4
36. Cho SA, Jung SK (2003) A removal torque of the laser-treated titanium implants in rabbit tibia. Biomaterials 24(26):4859–4863
37. Faeda RS, Tavares HS, Sartori R, Guastaldi AC, Marcantonio E Jr (2009) Biological performance of chemical hydroxyapatite coating associated with implant surface modification by laser beam: biomechanical study in rabbit tibias. J Oral Maxillofac Surg 67 (8):1706–1715. doi:10.1016/j.joms.2009.03.046
38. Silva NR, de Souza GM, Coelho PG, Stappert CF, Clark EA, Rekow ED, Thompson VP (2008) Effect of water storage time and composite cement thickness on fatigue of a glass–ceramic trilayer system. J Biomed Mater Res B Appl Biomater 84 (1):117–123. doi:10.1002/jbm.b.30851
39. Zarb GA, Schmitt A (1990) The longitudinal clinical effectiveness of osseointegrated dental implants: the Toronto study. Part III: problems and complications encountered. J Prosthet Dent 64 (2):185–194
40. Naert I, Quirynen M, van Steenberghe D, Darius P (1992) A study of 589 consecutive implants supporting complete fixed prostheses. Part II: prosthetic aspects. J Prosthet Dent 68(6):949–956
41. Pylant T, Triplett RG, Key MC, Brunsvold MA (1992) A retrospective evaluation of endosseous titanium implants in the partially edentulous patient. Int J Oral Maxillofac Implants 7(2):195–202
42. Gunne J, Jemt T, Linden B (1994) Implant treatment in partially edentulous patients: a report on prostheses after 3 years. Int J Prosthodont 7(2):143–148
43. Lekholm U, Gunne J, Henry P, Higuchi K, Linden U, Bergstrom C, van Steenberghe D (1999) Survival of the Branemark implant in partially edentulous jaws: a 10-year prospective multicenter study. Int J Oral Maxillofac Implants 14(5):639–645
44. Henry PJ, Laney WR, Jemt T, Harris D, Krogh PH, Polizzi G, Zarb GA, Herrmann I (1996) Osseointegrated implants for single-tooth replacement: a prospective 5-year multicenter study. Int J Oral Maxillofac Implants 11(4):450–455
45. Adell R, Lekholm U, Rockler B, Branemark PI (1981) A 15-year study of osseointegrated implants in the treatment of the edentulous jaw. Int J Oral Surg 10(6):387–416
46. Goodacre CJ, Kan JY, Rungcharassaeng K (1999) Clinical complications of osseointegrated implants. J Prosthet Dent 81(5):537–552